Canon printer carriage

4GB00, Computer Aided Engineering - Q1 (2024)

Group 10

Full Name	**Student ID**
[redacted]	[redacted]
Tobias Wejbora	
[redacted]	

Tutor: Priyam Dayora

Eindhoven, March 23, 2026

Contents

Executive summary

The report presents the development and optimization of the Canon COLORADO 1650 printer carriage design aimed at improving dynamic stability and minimizing resonance, aligned with efficient manufacturing and performance requirements. External components of the printer cause vibrations at the printer's operating frequency of 50Hz. Thus, the primary goals of this report include achieving eigenfrequencies above 50 Hz, with no resonance peaks in the Bode plot below 75 Hz in order to prevent external vibrations near the system's operating frequencies.

The design process focused on achieving a balance between structural integrity and manufacturability, targeting mass production at low cost. The initial analysis involved assessing areas of structural weakness and optimizing connections through RBE2 elements to explore the viability of the design and configurations for improving eigenfrequencies. If these RBE2 elements proved to be beneficial, parts were designed out of sheet metal and metal tubes to mimic the theoretical elements. Materials with high stiffness-to-density ratios, like steel, were selected due to their stability, while the use of simple sheet metal manufacturing techniques was used due to their cost-effective production and assembly.

The final design met most frequency response and all mass requirements, verified through eigenfrequency analysis, frequency response functions (FRFs), and mesh refinement studies. With comprehensive testing and many iterative design adjustments, the optimized carriage effectively solves the vibration-induced disturbances, ensuring high print accuracy.

1 | Introduction

The primary objective of this report is to design and modify the COLORADO 1650 printer carriage that meets the specific dynamic requirements. While components from the old carriage will be reused, or remain unedited, the rest must be redesigned to ensure optimal and improved performance. The design will be based on two key criteria that must be met: first, all eigenfrequencies of the carriage must be above 50 Hz to ensure stable dynamic behaviour. Second, the reaction of the print heads to two defined disturbances should show no peaks in the Bode plot below 75 Hz, minimizing the effect of actual disturbances due to contact points with surrounding elements. Peaks may indicate problematic resonances from disturbances caused by surrounding machine components. Multiple vibration sources within the machine, such as bearings, print carriage motors, curing carriage motors, and a chiller unit, all contribute to a natural frequency of 50 Hz. To prevent resonance between these vibration sources and the natural frequencies of the carriage, the design must focus on creating a mismatch in frequency and displacement.

To achieve this, the design aims to minimize the use of expensive manufacturing techniques, such as milling, turning, sheet metal, and plastic injection moulding, ensuring that production remains cost-effective for approximately 1000 units per year. By simplifying geometries and parts, the design reduces manufacturing complexity, cost, and assembly time, while maintaining a balance between functionality, cost, quality, and time. Whenever possible, parts from the previous carriage design are reused to streamline assembly and maintenance. Additionally, the design must ensure stability and damping, particularly in the y-direction, to reduce disturbances like dot mispositioning. The printhead should be lightweight to enhance performance without compromising structural integrity, and a high precision drop position accuracy of 15 µm is targeted, although this is a challenging goal. There is also a stretch goal of achieving a 5–10% improvement in printing speed.

Considering the physical constraints, the design ensures all eigenfrequencies are above 55 Hz, which provides an approximate 10% margin of safety. To achieve this, soft springs were replaced with RBE2 elements in simulations to evaluate the feasibility and structural integrity of the carriage design. Additionally, special attention was given to the dynamic behaviour of the carriage, ensuring that the two Bode plots for input points show clear and acceptable behaviour within the 10–80 Hz range.

A three-step design process was followed: first, improving the carriage design while adhering to the specific manufacturing, material, and physical constraints. The full requirements and constraints can be found in the appendix (see Appendix A). The manufacturing techniques considered include milling, turning, sheet metal work, and plastic injection moulding, ensuring that the design remains cost-effective for production volumes of approximately 1000 units per year.

Eigenfrequency analyses and Bode plots were run to verify whether our design meets the dynamic requirements, with iterations as needed. Finally, a mesh refinement study was conducted to validate the accuracy of the results.

The ultimate goal is to create a mismatch between the carriage's natural frequency and the disturbance sources at 50 Hz, ensuring stable dynamic performance with minimal vibration effects on the printheads.

2 | Analysis of the problem

For the analysis of the problem, the primary challenge in designing the carriage lies in managing its dynamic behaviour to avoid resonance with external vibration sources. The problem arises because the carriage is exposed to various vibration sources, such as bearings, the print carriage motor, the curing carriage motor, and other components. These introduce disturbances near the natural frequency of 50 Hz. This overlap between external vibration frequencies and the natural frequencies of the carriage creates a potential for dynamic instability during printing, leading to issues like mispositioning of dots in the y-direction during printing, as well as worsened overall print quality.

The most concerning resonance frequency, 50 Hz, corresponds to the natural frequency of the system. If the carriage's natural frequencies align with the 50 Hz source, excessive vibrations will go through the system, leading to significant mechanical disruptions. These disruptions include inaccurate positioning of the printhead, inconsistent dot placement, and potential damage to sensitive components. The objective is to create a frequency mismatch, where none of the carriage's eigenfrequencies fall below or close to 50 Hz, thereby eliminating resonance. This frequency mismatch must be carefully thought through while ensuring that the carriage remains structurally sound.

Furthermore, It must be ensured that the Bode plot, which represents the system's response to disturbances over a range of frequencies, shows no significant peaks below 75 Hz. Any peaks below this threshold would indicate areas where vibrations could negatively affect the print quality, potentially leading to printhead oscillation or excessive vibrations that further degrade the output. Therefore, the goal is to create a smooth Bode plot response without significant peaks of external disturbances below 75 Hz.

Another important factor in the design is the interaction of surrounding components, which can exacerbate the resonance problem. The carriage is not operating in isolation but is surrounded by multiple vibration sources, each of which can induce resonances or interact with the natural frequencies of the carriage. These interactions must be carefully analyzed. Eigenfrequency analysis will identify the natural frequencies of the carriage, while Bode plot analysis will assess the impact of disturbances on system performance.

The requirements, preferences and constraints are factors that make it more difficult to introduce design changes aimed at solving the resonance issue, as every change must be carefully assessed in terms of both its dynamic and structural impacts.

The solution, therefore, involves strategically modifying and replacing components to shift the natural frequencies of the system, ensuring that none fall near 50 Hz while still maintaining the overall structural integrity and performance of the carriage. One approach involves stiffening certain elements of the design. Additionally, by replacing soft springs with stiffer elements or RBE2 elements in simulations, It can be evaluated how design changes affect both the eigenfrequency and dynamic response of the carriage. This iterative process allows for the continuous refinement of the design until the resonance issue is fully fixed, resulting in a carriage that meets the dynamic requirements.

3 | Design Strategy

A well-thought-out design strategy is essential to achieving the desired outcome. The goal is to develop a solution that balances execution speed, product quality, and ease of manufacturing. The strategy should focus on optimizing key areas of the model to produce a high-quality, easily manufacturable product within the shortest possible time without extensive trial and error.

A comprehensive analysis of the provided model is crucial. This includes identifying which eigenvalues require improvement to reach the minimum target frequency of 50 Hz. Each eigenfrequency corresponds to a specific mode shape, which describes the deformation pattern of the structure at that frequency. By means of special software, it is possible to carefully examine these deformation patterns. Therefore, it becomes possible to determine locations with large amounts of bending or torsion. This information is essential for designing components aimed at increasing the eigenfrequencies.

3.1 | RBE2 Element Analysis

RBE2 elements play a crucial role in the early stages of the design process. Insights gained from the initial model analysis help to identify which parts of the model show movement or deformation and in which direction. To counteract these, RBE2 connections will be established between components. These massless infinitely stiff elements are ideal for increasing eigenfrequencies. They allow for rapid exploration of different connection strategies, quickly identifying which connections most effectively enhance eigenfrequencies. These connections will be designed with the potential to be transformed into physical parts, considering any restrictions or areas where adding parts is not permitted.

Various configurations of RBE2 connections between points in the model will be tested. Using this approach, fast simulations can be conducted to evaluate the impact of these connections on the model's eigenfrequencies. For instance, as shown in Figure 3.1, two components can be connected in various ways.

Using either the purple or blue connection will produce different results. The optimal part design is thus determined through simulations, with the preferred option being the one that reaches the highest eigenfrequencies.

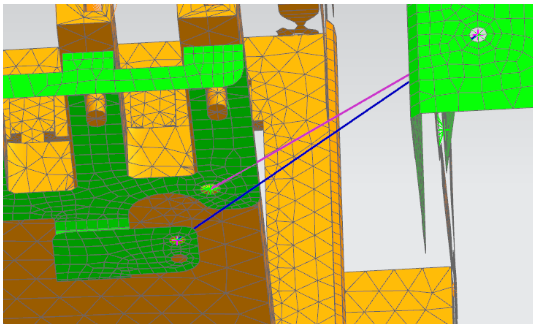

Figure 3.1: Different RBE2 connections

3.2 | Carriage Design

Now that the optimal connections can be identified, the next step is to devise a strategy for the carriage design. The main goal is to increase the carriage's eigenfrequencies to a safe level while maintaining manufacturability and cost-efficiency. A thorough analysis is important to ensure that the detailing phase of the design produces good results and to prevent serious setbacks in the later stages of the project.

Material selection

One of the most important decisions in carriage design is material choice. The relatively narrow list of available materials allows for already making a certain decision. Generally, a stiffer carriage would increase natural frequencies, while a higher mass would decrease them. Therefore, the first characteristic that potential materials should be compared upon is the stiffness/density ratio or formally the E/ρ ratio, where E is the material's Young's modulus and ρ the density. E/ρ has a strong positive correlation with the eigenfrequencies of the carriage. Steel and aluminium have similar E/ρ values, which are much higher than for standard polymers to which PC, ABS, and their glass-filled variants belong (Figure A.3). For example, for steel and aluminum E/ρ varies between 25-35GPa/(g/cm^3), while for PC it is approximately 2GPa/(g/cm^3). Therefore, the choice lies between the above two metals.

Since E/ρ values are very close for steel and aluminum, another factor decides the choice. The carriage should bear the relatively significant weight of the print heads, which is a fixed mass. The stiffer the material of the carriage the better it will hold it in place. The eigenfrequencies will thus be higher due to the increase in the stiffness/mass ratio of the whole carriage including the print heads. Therefore, the initial carriage and the newly designed parts should be made out of steel, which is much stiffer than aluminum [4].

Manufacturing & Cost-effectiveness

Due to the complex shape of the carriage, at least a moderate degree of flexibility in the customization of parts should be available to the group. On the other hand, a cost-efficient manufacturing process is sought. To balance out the above two factors it is important to keep the shape of each part as simple as possible and ensure a single simple manufacturing process [8]. The choice of manufacturing techniques is crucial to meet the above scopes. The available techniques were reviewed, which allowed the group to find the best option, which is discussed below. For the reasoning behind the rejection of other techniques please refer to Appendix A.2.

Sheet metal fabrication is a set of manufacturing techniques used in combination in a single factory (1 supplier possible). It allows a higher design flexibility and high-volume production, which will reduce costs if parts are ordered in bulk. The costs can also be managed by carefully choosing the manufacturing steps and type of techniques to use in the process. We strive to use the simplest techniques and minimize the number of production steps. The first step to achieve that is minimizing the features of parts to necessary ones: bolt holes, 90-degree bends, and custom cuts like part outlines and weight reduction cutouts [8].

Holes should be of similar size to reduce costs, and punching can be used, which offers high accuracy. The bends can be made with bottoming with a V-die or with folding [3]. Both techniques offer high precision and low production costs. Lastly, cutouts can be made with either water, laser, or plasma cutting. The cheapest and least accurate one is the plasma cutting for which the typical kerf width is +3.8mm and the tolerances for manual and CNC types are around 1.6mm and between 0.38 to 0.64 mm, respectively [2] [5] [1]. These deviations can be accounted for by leaving safety margins. Manual cutting will be used for as many parts as possible to reduce costs. Therefore, the above-described sheet metal fabrication process will be used for all parts.

Now that the costs of machining have been discussed, another important consideration is the costs of raw materials. We will use 1.5mm sheet thickness to increase stiffness. 1mm sheets will only be used if the weight limit is reached. Fortunately, 1.5mm cold-rolled sheet steel is considerably cheaper than 1.5mm sheet aluminium, which aligns with the above-mentioned material choice [7] [6].

Part Geometry & Stiffness

The designed part must be able to withstand the forces and bending moments acting on it. Choosing the right geometry is critical. For instance, using U-shaped or L-shaped beams (Figure A.2) can provide better resistance to bending forces, ensuring structural integrity. Since we strive for a simple shape, beams with homogeneous cross-sections with high second moments of inertia are a great choice. Such parts can be easily made with the chosen manufacturing process.

The simplest type of a beam is a rectangular beam (Figure A.1). Due to the limitations of the chosen manufacturing technique, one of the sides will be 1.5mm long and the other can be much longer, which will only allow high bending stiffness for 1 bending axis. One of the least weight-increasing solutions is an L-beam (Figure A.2), which provides high bending stiffness for both axes. Moreover, for sheets longer than just 9mm the bending stiffness of an L-beam is greater for the straight sheet in its strongest bending direction (Appendix A.2). The torsional effects can be mitigated by making firm connections with bolts onto the body of the carriage and by adding parts in different locations in the carriage to increase its rigidity.

3.3 | Verification & Detailing

Once all the parts have been designed, simulations will be conducted. The simulation results will allow for the generation of eigenfrequencies and Bode plots. This information will be used to verify whether the model complies with the specified requirements. If necessary, the components can be modified to enhance performance until the design fully meets the requirements.

If all the designed sheet metal parts together cannot provide sufficient stiffness, the next best option regarding stiffness/cost ratio will be chosen. Therefore, hollow or filled tubes will be used, which can be thicker than sheet steel and thus provide higher bending stiffness. Epoxy glue will be used to connect them to the carriage. If necessary, threadless holes will be drilled manually (to avoid complex shapes), and glue will be used to hold the bolts in the holes.

4 | Final Design

In the following section, an insight into the design process and the underlying thought process involved in the creation of the parts is presented. It aims to provide a comprehensive understanding of the decisions made throughout the design process and how they contribute to the performance and functionality of the final assembbly created. The exploded view of the final design can be seen in Figure 4.1 with every part labeled.

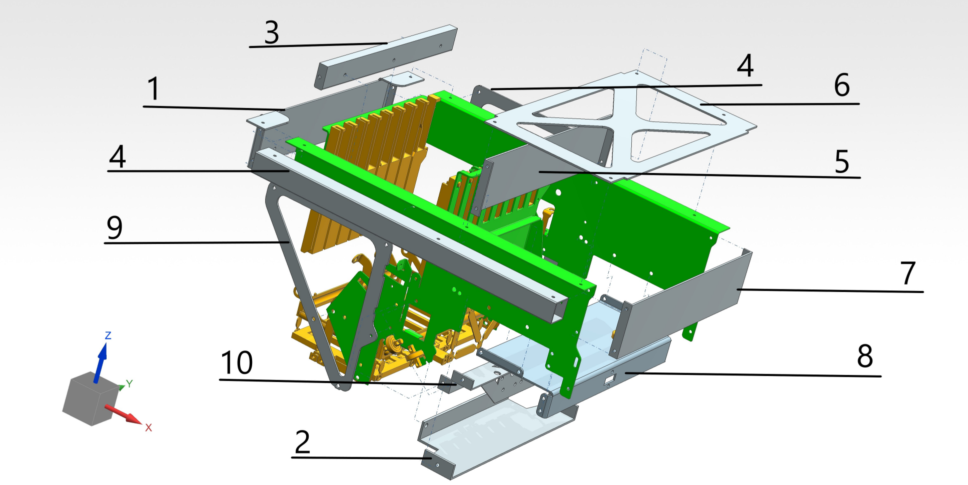

Figure 4.1: Exploded view of assembly

Parts 1, 3, 4 and 9

These parts are designed to enhance the structural integrity of the printer carriage by connecting key components and preventing misalignment. Part 1 connects the two side plates to the front centre printer head module, reinforcing the structural alignment of the carriage. This helps reduce rotation around the X-axis and prevents compression along the Y-axis, both of which are crucial for improving print quality. Parts 4 and 9 provides additional compressional support along the Z-axis and prevents rotation around the Y-axis. By linking the side plates to the top of the carriage, it reinforces the framework, ensures better load distribution, and minimizes potential misalignment. Together, these parts work to stabilize the entire printer carriage.

Parts 2, 5 and 10

The middle part addresses the need for better stability and improve load distribution within the structure. By extending the middle part and incorporating an additional attachment point where the hinges would normally be, the design takes the load off the hinge system from the side, resulting in greater rigidity. This reduces any play or movement, which improves the printing quality of the carriage, particularly in modes that are sensitive to lateral instability (modes 9 and 10).

Parts 6 and 7

This part was created with the idea of maintaining the structural integrity of the printer carriage. It was designed to strengthen the structure and resolve side plate buckling/displacement issues. Enclosing the lateral plates and extending them internally, significantly increases assembly rigidity, raising the natural frequency in Mode 7 and improving dynamic printing stability. The design idea of having both external and internal support in order to generate a balancing dynamic performance with structural stability.

Part 8

This part was created to secure the bearing to the lower center of the model, tackling the need to control rotational and compression forces. Its primary function is to resist rotation around the Z and X axes, particularly important for stabilizing the carriage during printing. The L-shaped shape of this part was made with the idea of preventing undesired movements, thus contributing to the precise performance of the printer carriage.

4.1 | Final Carriage Design and Eigenmodes

The finalized cartridge design, incorporating all the components discussed in previous sections, is illustrated in Figure Figure 4.2. The green and orange parts were provided by the course, while the grey parts represent those described earlier. After assembling the final cartridge, the eigenvalues were computed, and the results are presented in Table 4.2. All eigenvalues should be above 50 Hz, while 2 of them should be above 75Hz. As can be seen in Table 4.2 all values are above 75Hz and modes 9 and 10 are even above 100 Hz, so the objective has been completed and even surpassed.

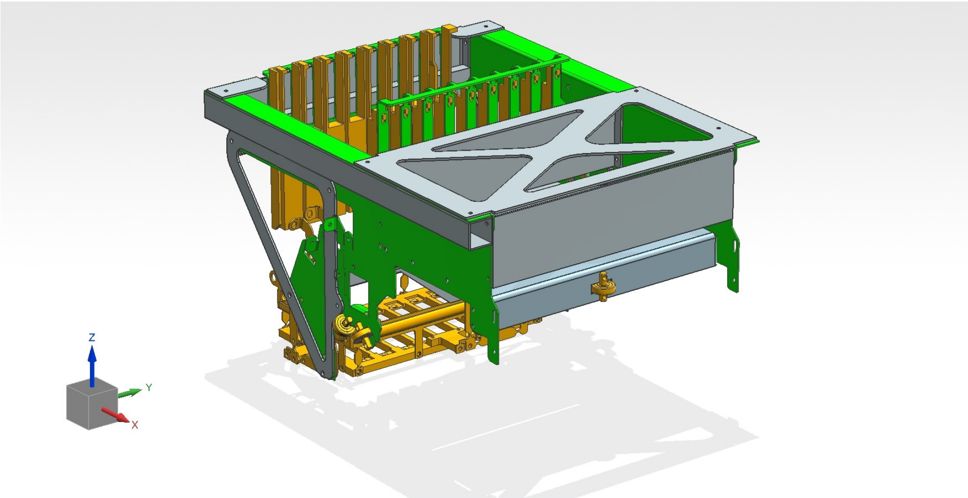

Figure 4.2: Final Cartridge Design

Part	Weight (kg)
1	0.1292
2	0.1984
3	0.0853
4 and opposite part	0.1284
5 and 7	0.1181 x2
6	0.1906
8	0.2269
9	0.1656
10	0.1019
Total parts.	**1.4624**

Table 4.1: Weight of parts

Mode 7	81.37
Mode 8	94.92
Mode 9	113.21
Mode 10	116.40

Table 4.2: Eigenvalues of the model

4.2 | Mass

Considering the additional parts, a weight restriction of 1.5 kg was imposed. The mass of each part was determined using the Siemens NX analysis tool, and the total mass is displayed in Figure Table 4.1. The total weight remains within the 1.5 kg limit. The mass is near the limit, it was however chosen to make the model as stiff as possible instead of as light as possible.

4.3 | Frequency Response Function (FRF)

In addition to looking at the eigenvalues and mass, the Frequency Response Function (FRF) of the carriage, can be used to see the displacement-over-displacement and displacement-over-force magnitude over a range of frequencies, including frequencies at which the carriage operates. The displacement over displacement transfer function is chosen to analyse the rear bearing which undergoes runout, an enforced displacement. The displacement over force transfer function is used to investigate the force applied by the hoses attached to the side of the carriage. The results can be seen respectively in Figure 4.3 and Figure 4.4.

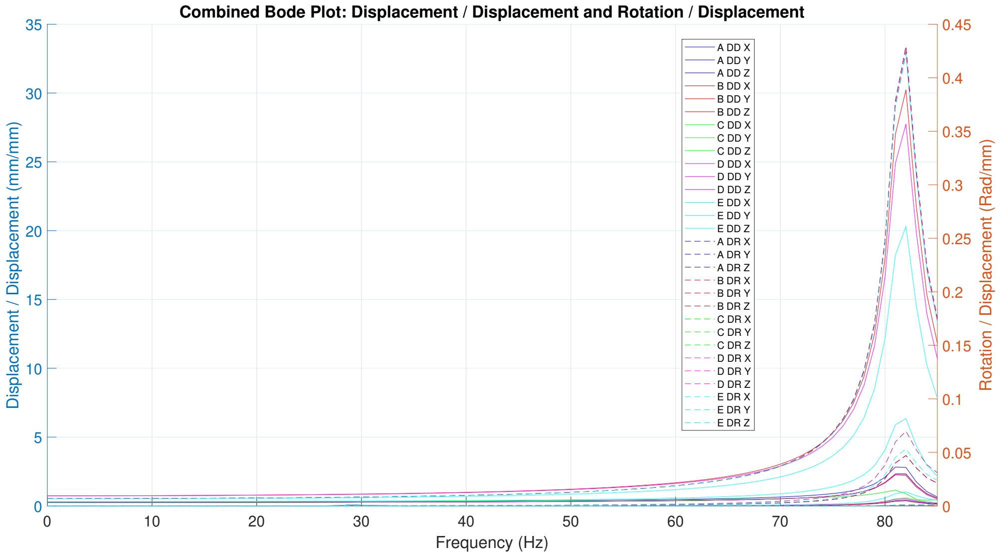

Figure 4.3: FRF: Displacement over Displacement

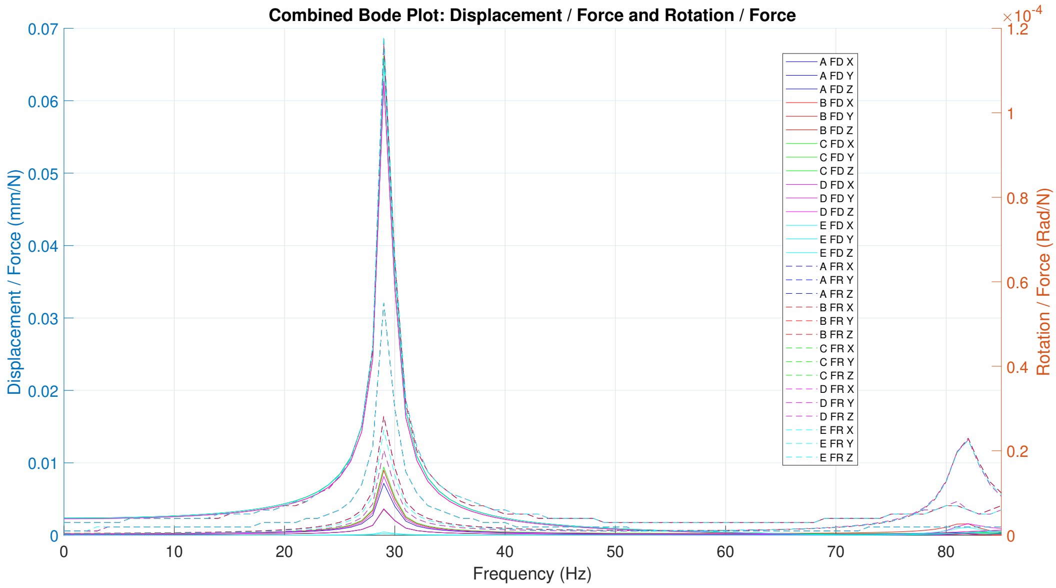

Figure 4.4: FRF: Displacement over Force

The target of having no peaks in the bode plot under 75Hz is only met for the displacement over displacement transfer graph as there is a prominent peak at 30Hz in the displacement over force graph. This peak was analysed by looking at the displacement at 30Hz which shows high y-axis displacement at the printer head alignment plate above the printer head matrix plate. To counteract this high displacement, a beam was placed to stiffen the area and the whole carriage in the y direction. This did not shift or mute the peak at 30Hz, therefore, the issue was narrowed down to mass distribution. To increase the eigenfrequency, the mass can be removed from the printer head area, however, this could not be done without sacrificing the eigenmode frequencies. The displacement over force peak reaches close to 0.07 mm/N meaning that if a force of 1 Neuton can be assumed to be applied by the hoses, then a displacement of 0.07mm can be observed. Comparing this to the recognized original 20mm print head displacement at 50Hz the magnitude of displacement caused by the peak at 30Hz is of magnitudes lower. Nevertheless, during operation, the printer head will operate at 30Hz while accelerating thus the peak at 30hz will still prevail as an issue.

5 | Verification of FE results for the final design

5.1 | Mesh Refinement Study

To ensure the accuracy of the Finite Element Method (FEM) analysis, a mesh refinement study has been executed to determine the most efficient mesh size for eigenvalue computation. When the mesh sizes decrease, the results of the FEM simulations approach towards the most accurate solution. However, smaller mesh sizes also increase the computational power and time.

Various mesh sizes were selected between 40 mm to 1 mm. The step size between mesh sizes 40 mm to 5 mm was 5 mm, while a smaller step size of 1 mm was used between 5 mm and 1 mm. With a decreasing mesh size, the number of elements in the model increases, resulting in a more complex simulation with more computation time. The eigenvalues obtained from the simulations for the different mesh sizes and modes (modes 7 to 10) are stated in Table 5.1.

mode/n	40	35	30	25	20	15	10	5	4	3	2	1
Mode 7	58.91	58.87	58.14	57.61	57.49	57.35	57.17	57.06	57.04	57.04	57.04	57.06
Mode 8	92.44	92.28	92.23	92.09	92.05	91.98	91.92	91.86	91.85	91.85	91.84	91.83
Mode 9	105.73	105.07	105.05	104.72	104.75	104.58	104.4	104.34	104.33	104.32	104.32	104.31
Mode 10	112.48	112.44	112.27	111.94	111.83	111.62	111.35	111.17	111.16	111.15	111.14	111.13

Table 5.1: Modes and corresponding eigenvalues (Hz) for different mesh sizes (n)

To better visualize the effect of mesh refinement on eigenvalue accuracy, the eigenvalues were normalized. The normalization allows for easier comparison between different mesh sizes. The normalized eigenvalues were computed using the following equation, where λ_{max} and λ_{min} represent the maximum and minimum eigenvalues for each mode:

$$\lambda_{\text{normalized}} = \frac{\lambda - \lambda_{\text{min}}}{\lambda_{\text{max}} - \lambda_{\text{min}}} \tag{5.1}$$

The normalized eigenvalues for the different modes and mesh sizes are plotted in Figure 5.1. The plot highlights the convergence of the eigenvalues as the mesh size decreases.

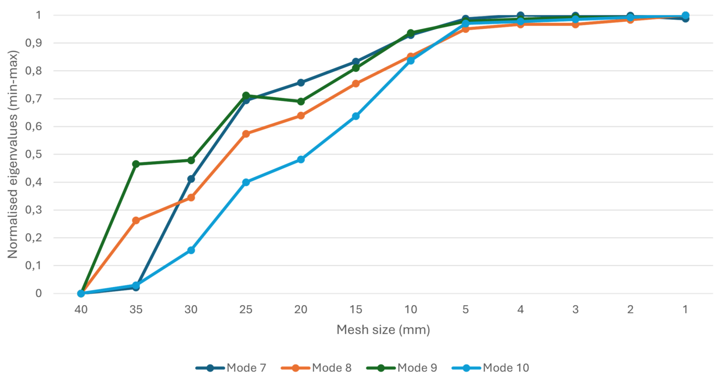

Figure 5.1: Normalized eigenvalues for decreasing mesh sizes

5.2 | Analysis of Results

The plot in Figure 5.1 shows a clear trend: as the mesh size decreases from 40 mm to 5 mm, the slope of all the different modes decreases, indicating an approach of the most accurate results. For mesh sizes smaller than 5 mm, the eigenvalues converge even more but only with a minimal difference. The improvement in accuracy becomes almost negligible. For mesh sizes between 3 mm and 1 mm in the table (Table 5.1), the maximum difference between eigenvalues is less than 0.02, which translates to an error percentage of less than 0.05. This is sufficiently small for this case. Next to this, the time required to simulate eigenvalue calculations for mesh sizes 3 mm or smaller remains under 5 minutes, showing that this mesh size is still viable.

5.3 | Bode plot quality

The resolution of the Bode plot has been set to 1 Hz to ensure that no significant peaks are overlooked. This level of precision was also recommended by the course instructors to ensure an accurate analysis. The mesh refinement study shows that a mesh size of 3 mm is sufficient for accurate eigenvalue calculations. Having a lower mesh size, such as 2 mm or 1 mm, offers only minor improvements in accuracy while demanding more computing power. Therefore, mesh sizes smaller than 3 mm are not necessary for this case.

6 | Manufacturing Plan

This chapter contains the manufacturing plan, focusing on creating cost-effective parts and creating a simple assembly process. The specifications and manufacturing techniques of the parts are discussed, as well as the method of assembling the parts is explained.

6.1 | Manufacturability of parts

It is visible in Figure 6.1 that all the parts created consist of bent or cut sheet steel. Using only simple sheet metal manufacturing techniques reduces the complexity and cost of the manufacturing process without losing much performance or room for creativity in the part design, as can be read in section 3. All the parts in the assembly are cut using laser, water or plasma cutting, and are bent using folding techniques. For bending the parts an inner radius of 1.5, and an outer radius of 1.5mm is used. Holes are created in the newly created parts, as well as in some parts of the carriage by punching. These holes have a uniform size of 3mm to simplify the assembly process. Two beams are ordered separately instead of using sheet metal fabrication because otherwise welding would be needed (ADD NUMBER OF PART HERE)

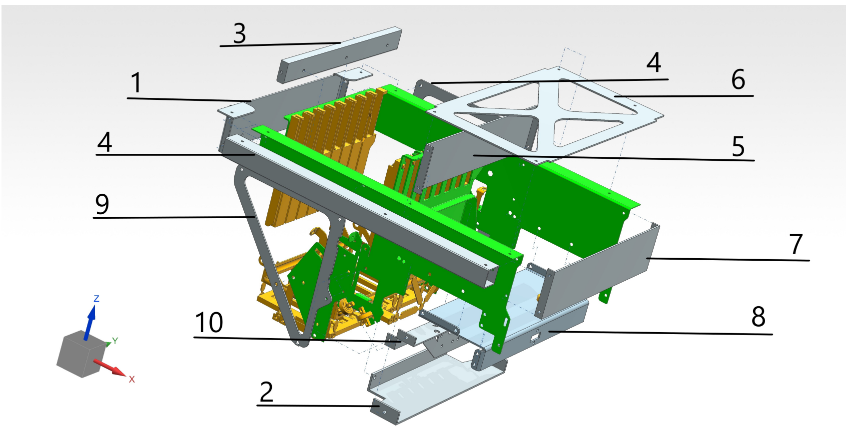

Figure 6.1: Exploded view of assembly

6.2 | General Assembly process

It is an important aspect of the manufacturing plan to describe the ease of assembly. This subchapter describes how the parts will be fitted onto the carriage and which changes have to be made to the carriage. Bolts, nuts, and washers are used to hold most of the parts in place. Washers were added to distribute the load on the bolts and nuts more evenly. The reason that bolts were generally chosen over glue is due to their superior durability and strength. Connections with bolts and nuts also provide a stiffer connection than glue. A disadvantage of using bolts is that the holes needed for it can weaken the material. Another difficulty with bolts could be that in some parts it could be hard to fasten the bolts, but this is only the case for 2 parts that the group created. These are parts 3 and 4. For these parts glue will be used to attach it to the carriage. To reduce the cost needed for the bolts, and to simplify the assembly process, a single nut, bolt, and washer size was chosen. The holes throughout the entire carriage are 3mm so 3M bolts are selected. Since this is the only method of attaching parts to the entire carriage, the bolts, nuts, and washers can be ordered in bulk, which will be cheaper.

7 | Conclusion and Evalutation

7.1 | Conclusion

In conclusion, by implementing the design plan and manufacturing steps to produce the necessary parts highlighted in this report, the design objective of steering the natural eigenfrequencies of the printer carriage away from 50hz is met. The system's response to external disturbances caused by the other parts of the printer occurs at frequencies over 30Hz as seen in Figure 4.4, thus, the force exerted by the hose/s is the limiting factor. The results displayed in this report were achieved by analysing the carriage dynamics and identifying areas of structural weakness at each mode shape. Furthermore, RBE2 elements were placed in areas of high displacement at the natural frequencies of the carriage. These RBE2 elements confirm whether introducing a new part is beneficial to increasing the eigenfrequencies of the carriage. When areas of importance are found, manufacturable parts made out of sheet metal have been designed and added to the assembly to ensure that all parts integrate seamlessly. The use of simple sheet metal fabrication methods like bending, cutting and punching, results in a cost-effective manufacturing process. Moreover, sheet metal in combination with the choice of steel as the metal material provided the carriage with an optimal stiffness-to-mass density ratio. When higher stiffness was required for areas of high displacement, steel tubes were used. These design choices allowed the dynamic performance goals to be met and for the total mass addition to be under 1.5kg. The rear bearing and the mass of the printer head were identified as parts of the carriage of high importance. Firstly, the rear bearing undergoing run-out causes an enforced displacement in the magnitude of 10^{-6}, meaning that within the range of operating frequencies, the magnitude of error should be lower in magnitude to ensure minimal displacement at the printer head matrix. Finally, a mesh refinement study has been performed to validate the FEM results. A mesh size of 3mm provided a sufficient balance between computational energy and error, resulting in an error percentage of less than 0.05.

7.2 | Evaluation:

FRF graphs have been used to analyse carriage dynamics of the two input variables over a range of frequencies. The magnitude of abnormal peaks in the displacement/displacement or displacement/force was targeted by identifying the deformation at these frequencies and designing parts to stiffen these areas. The results of the displacement over displacement FRFs show a peak at 83Hz, while the displacement over force FRF shows a stubborn peak at 30Hz. Analysing the displacement at this frequency, the printer head modules were undergoing high deformation which was a difficult region of the carriage to stiffen. This displacement stems from the force disturbance created by the external hose/s. The displacement transfers through the carriage to the area of high mass, being the printer head. Therefore stiffness and mass distribution modifications were made however, the peak still prevailed. Therefore, the modifications made to the printer carriage design partially meet the primary objectives ensuring that all eigenfrequencies are above 50Hz and that there are no resonance peaks below 75Hz in the FRFs.

How AI used in the report

Throughout the course, no AI was used to generate any parts or figures related to the assembly. However, AI tools were employed to review and improve the clarity, grammar, and professional writing style of the text in the report. Most importantly, no content was created, generated, or produced by AI. The AI tools were used solely for proofreading and refining pre-existing text made by team members to improve its quality.

8 | References

[1] Mike Best. A guide to mechanized plasma cutting. https://www.thefabricator.com/thefabricator/article/plasmacutting/a-guide-to-mechanized-plasma-cutting#:~:text=However%2C%20the%20general%20tolerance%20for,%C2%B10.015%20to%200.020%20in., 2019. Accessed: 2024-10-23.

[2] Swanton Welding Company. Plasma vs. laser vs. water cutting. https://swantonweld.com/plasma-vs-laser-vs-water-cutting/. Accessed: 2024-10-23.

[3] Ecoreprap. 7 types of sheet metal bending you should know. https://ecoreprap.com/sheet-metal/types-of-sheet-metal-bending/. Accessed: 2024-10-23.

[4] Engineers Edge. Densities of metals and elements table. https://www.engineersedge.com/materials/densities_of_metals_and_elements_table_13976.htm. Accessed: 2024-10-25.

[5] Hypertherm. How accurate is plasma and what kind of cut and edge quality can i expect? https://www.hypertherm.com/resources/spark-the-blog/how-accurate-is-plasma-and-what-kind-of-cut-and-edge-quality-can-i-expect/, 2019. Accessed: 2024-10-23.

[6] Limtrade. Aluminum sheet plates cost. https://www.limtrade.nl/aluminium-plaat-2000x1000x1-5-mm-1050a-h14-h24. Accessed: 2024-10-23.

[7] Limtrade. Steel sheet plates cost. https://www.limtrade.nl/kgw-plaat-2000x1000x1-50-mm-kgw-plaat. Accessed: 2024-10-23.

[8] RapidDirect. Top tips for reducing sheet metal fabrication cost. https://rapiddirect.medium.com/top-tips-for-reducing-sheet-metal-fabrication-cost-831962d755ef, 2023. Accessed: 2024-10-23.

A | Problem analysis & Design strategy - Details

A.1 | RPC

Requirements

- Ensure all carriage Eigenen frequencies are above 50Hz (with a target of 55Hz to provide a 10% margin).
- Ignore the 6 modes around 0Hz in Eigen frequency analysis.
- No resonance peaks in the Bode plot below 75Hz to avoid excessive vibrations.
- Analyze and mitigate the reaction of printheads to two specific disturbances (no peaks below 75Hz in the Bode plot).
- Define and avoid significant peaks in the dynamic response that could affect stability or performance.
- Use materials such as steel, aluminum, PC, ABS, and their glass-filled versions for sheet metal, shafts, and structural components.
- Replace soft springs with RBE2 elements in simulations to evaluate design feasibility and structural integrity.
- Ensure the model successfully runs through Eigen frequency analysis and Bode plot simulations with accurate and valid results.

Constraints

- Design for mass production using standard manufacturing techniques such as milling, turning, sheet metal fabrication, and plastic injection molding.
- Sheet metal thickness: 0.5–2 mm (steel or aluminum).
- Tube or shafts: Steel or aluminum.
- Plastic components: PC, PC Glass Filled, ABS, or ABS Glass Filled.
- Total carriage weight must not exceed 1.5 kg.
- No parts should cross red boundaries in the CAD model (geometric constraints).
- Only attach parts to the green spiders at specific points, as defined in the FEM CAD model.

A.2 | Design strategy

Manufacturability & Costs

Little use can be seen in turning which produces radially symmetric parts. CNC milling is too expensive and will not be used. Manual milling could be used to make simple parts. However, it would be difficult to scale such a process. Therefore, pre-made parts like tubes could be used in combination with milling to drill necessary bolt holes, for example. Such a process would offer very limited customization flexibility and most likely involve at least 2 different suppliers, which could drive the costs and lead time up.

Geometry & Stiffness

In addition to symmetry effects, an L-beam has a higher second moment of inertia than a straight sheet (rectangular beam). The formulae for second moments of inertia for an L-beam and a rectangular beam, respectively, are the following:

$$I_x = I_y = \frac{t(5L^2 - 5Lt + t^2)(L^2 - Lt + t^2)}{12(2L - t)} \tag{A.1}$$

$$I_x = \frac{bh^3}{12};\ I_y = \frac{b^3h}{12} \tag{A.2}$$

Using these, it can be easily shown that if the sheet used is longer than 6 x thickness = 9mm, bending the sheet into a symmetrical L-shaped beam will make its second moment of area greater than the second moment of area of the strongest axis for the straight sheet. Most of the time the sheets used for parts will be longer than 9mm. The lengths of the sides might be different which will cause unequal second moments of area for each axis, though the above should be a sufficient demonstration of L-beam's potential. Therefore, L-beam or similar composite structures will be used as parts for the carriage.

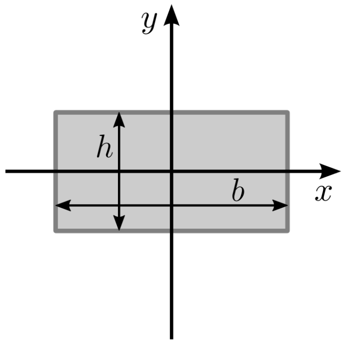

Figure A.1: Rectangular beam cross-section

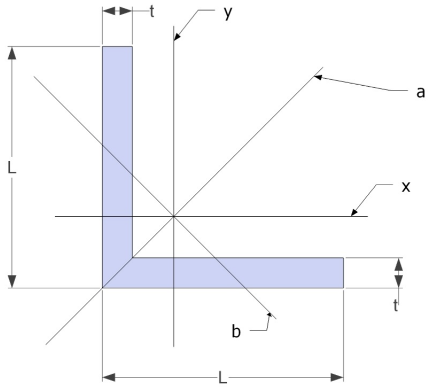

Figure A.2: L-beam cross-section

Material selection

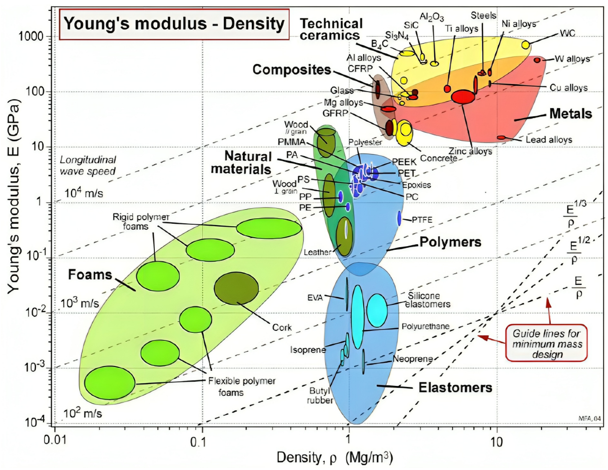

Figure A.3: E vs ρ chart for different materials

B | Parts design and manufacturing

B.1 | Parts removed from manufacturing plan

loose_bearing_p2.prt

This part connects the lower centre of the model to the bearing. This part can be created solely using sheet metal of thickness 1.5mm. The mounting connection bends have a radius of 3mm, meaning that this bend can be formed using a sheet metal press. The mounting holes are 3.2mm wide to allow a bolted connection to the existing model. The part is connected to the loose bearing through both bearing holes via a bolted connection. The part resists rotation in the Z axis in the centre of the model and given the L shape of the part, it also resists rotation in the X axis. Furthermore, this part limits compression in the x and y axis.

backpiecev3.prt

This part connects the two side plates of the model to the front centre printer head module. Mounting holes are placed on the flange of the side plates and on the inside of the side plates. Furthermore, it is connected to the centre printer head module with 4 bolts. This part reduces rotation around the x-axis and stops compression in the y-axis. The part is 1.5mm thick and the bends have a radius of 3mm.

back_side/back_side_left.prt

This part connects the side plates from the printer head matrix location to the top of the side plates. This part provides compressional support in the z direction as well as limiting rotation in the y-axis. The part is connected to multiple locations of the side plates via bolted connections. The part can be manufactured out of sheet metal and no bends are required.

B.2 | Manufacturability

Top part

From a manufacturability point of view, the part is designed with simplicity and efficiency in mind. Its features, such as plane surfaces and straightforward profiles, make it easy to produce using sheet metal. The internal and external wrapping elements are designed to be made from a single piece and assembled in a few simple steps, reducing overall production time and cost. Standardized holes (all around the carriage) simplify the assembly process, allowing for quicker integration into the final structure. This specific part would require welding only one component, while the remaining sections can be produced from the same sheet metal, making it easy and cost-efficient to manufacture.

Additionally, this part is made of steel, which is durable yet lightweight, ensuring that it contributes to stability without significantly increasing the carriage's weight—critical for maintaining the system's dynamic response and meeting the 1.5 kg maximum weight requirement.

Middle Part

The manufacturability of this part has been carefully considered. The middle part features relatively simple plane profiles, which make it well-suited for cutting processes such as laser cutting or milling. The inclusion of standard holes allows for easy assembly with the rest of the structure, minimizing the need for customization or complex tools.

The extended attachment points and removal of the hinges simplify the assembly process, reducing time. The cutouts not only decrease material costs but also ensure that the part can be manufactured using standard metal sheets, minimizing the use of costly and complex manufacturing processes. This design strikes a balance between structural performance and ease of production.

Back Part

The back part's updated design is well-suited for the allowed manufacturing techniques, optimizing production efficiency and lowering costs. The large triangular feature simplifies the design and makes it easier to machine. The design allows for precise milling of the triangular features, ensuring consistent dimensions across production.

The simplified triangular geometry makes the back piece ideal for sheet metal fabrication. Using laser cutting for the large triangle speeds up production and reduces material waste, cutting down overall production costs.